Investigating the Influence of Lateral Loading on the Vertical Capacity of Coal Mine Standing Supports

Khaled Mohamed, Morgan Sears, Timothy Batchler
CDC/NIOSH Pittsburgh Mining Research Division

ABSTRACT
The National Institute for Occupational Safety and Health (NIOSH) initiated a testing program to assess the effects of lateral loading on various standing supports used in underground coal mines. This study is not intended to endorse a particular type of standing supports nor to provide a comparison between different types of standing supports.

This paper aims to measure the lateral loading capacity of two types of standing supports and evaluate how it affects their vertical loading capacity and yielding mechanisms. The study utilizes the Mine Roof Simulator (MRS) at NIOSH Pittsburgh. Type-1 support is characterized by telescopic tubes made from ASTM A-513 steel with a specified locking mechanism, and Type-2 support comprises a single component constructed from ASTM A500 Welded Grade C pipe.

Vertical load tests were carried out to assess the designed performance of Type-1 and Type-2 props. Type-1 props demonstrated a "constant yielding" behavior, achieving an ultimate capacity of up to 140 kips. Type-2 props showed a "load shedding" behavior, reaching peak vertical loads of up to 191 kips. Buckling analysis revealed that Type-1 props were not designed to buckle, and Type-2 props failed due to buckling rather than material yielding.

Under vertical pre-loading, lateral loading tests showed that Type-1 props can withstand about 9 kips, and Type-2 props can withstand about 10.79 kips of lateral load. This represents roughly 6% of their vertical loading capacities.

Testing props under lateral loads in addition to their intended vertical loads showed that the lateral loads could influence their loading mechanisms. Type-1 props did not exhibit the expected "constant yielding" behavior under lateral load but instead showed "load shedding" decreasing their rated vertical capacity by 70%. At high vertical pre-loading, Type-2 props demonstrated "constant yielding" behavior instead of the anticipated "load shedding," leading to a 60% reduction in their rated vertical capacity.

These findings provide valuable insights into the behavior of these props under different loading conditions, aiding in their efficient use and design in underground mining operations.

INTRODUCTION

In underground coal mines, a variety of standing supports are primarily utilized for roof support and, in some cases, to contain collapsed rib materials. Some common types of standing supports in coal mines are timber posts, wood crips, steel props and hydraulic props. Figure 1 shows steel set and posts that were used as secondary supports in a long-term track entry in a room and pillar coal mine. In instances where roof bolters are not accessible for rib bolting, alternative methods like standing support systems can be employed to support fractured rib brows (see Figure 2a) or to contain detached rib (see Figure 2b). When spalled rib sections lean on these standing supports, as shown in Figure 3, the standing supports provide lateral resistance, increasing rib confinement and impeding further rib failure. Neglecting the impact of lateral load on standing supports could yield unfavorable outcomes, as it could significantly influence their stability. Sometimes, timbers had been set adjacent to sloughed ribs, which did not control or prevent the ribs from falling (see Figure 4) where timber posts exhibiting buckling at varying heights and dislodged posts due to rib spalling. Additionally, dislodged standing supports could lead to serious incidents, such as one striking a miner, resulting in fatal injuries [1].

The effectiveness of standing supports in underground coal mines depends on various operational factors such as the type of supports used, the composition and thickness of roof and floor strata, mining depth, and the spacing and layout pattern of standing supports, the magnitude and direction of applied loads on the support, etc. These factors collectively influence the performance and reliability of standing support systems in ensuring underground safety and stability.

Figure 1. Steel set and posts in a track entry

Standing supports are typically tested under vertical loading conditions to determine their load-bearing capacity and stiffness. Spearing [2] utilized the Mine Roof Simulator (MRS) to evaluate the vertical capacities and stiffnesses of the Quik Stik and Ball Buster standing supports. The study revealed that the Quik Stik props were categorized as nonyielding supports, whereas the Ball Buster props were classified as yieldable supports. Chen et al. [3] introduced a mechanical yielding steel prop (MYSP) with a design similar to the Ball Buster supports. This prop was engineered to tolerate substantial deformation in the field. Unlike the Ball Buster props that use a single layer of ball bearings, the MYSP featured double-layer steel ball bearings. The double-layer design achieved a higher vertical loading capacity. Chen et al. [3] demonstrated that the vertical capacity of the MYSP props could be regulated by altering the yielding strength of the inner and outer tubes of the prop.

(a) (b)

Figure 2. Standing supports used to support rib brow and to confine rib slab

(a) (b)

Figure 3. Standing support constrains dislodged rib

(a) (b)

Figure 4. Buckled and dislodged timber posts in underground coal mines

To the best of the authors' knowledge, minimal research has been done to assess the effects of lateral loading on various standing supports used in underground coal mines. Previous research investigated the effect of lateral displacements (simulating floor heave) on wood crib stability by controlled biaxial displacement of full-scale wood crib supports [4]. Therefore, NIOSH researchers [5] initiated a testing program for different types of standing supports. Many standing support providers were contacted, and some of them were willing to supply samples of standing supports. This study is not intended to endorse a particular type of standing supports nor to provide a comparison between different types of standing supports. The program aimed to determine the lateral loading capacities of tested supports, assess the impact of lateral loads on their vertical loading capacity, and analyze their yielding mechanisms. The key factors affecting the behavior of standing supports subjected to lateral loading will be studied in this testing program. These factors include the type of standing support (steel and timber), support geometry (shape, dimension), support structure (single-component or multiple-components), spatial location of the lateral load along the support, and end-conditions of support (rock strength).

PROBLEM DESCRIPTION AND RESEARCH METHODOLOGY

This paper explores several important research questions regarding the lateral loading capacity of tested props. It investigates whether lateral loading influences the rated vertical loading capacity of the props and how it affects their yielding mechanism. The study measured the lateral loading capacities of two types of standing supports, Type-1 and Type-2, and evaluated the effects of lateral loads on their vertical loading capacity and yielding mechanisms.

The Type-1 prop is comprised of two telescopic tubes made from ASTM A-513 steel. The upper end of the outer tube has a beveled section as shown in Figure 5c. The lengths of inner tube and outer tubes are 36 in and 82 in, respectively. The inner and outer tubes have outer diameters of 2.897 in and 3.506 in, respectively, with wall thicknesses of 0.270 in each. Both ends of the inner and outer tubes are attached with 8-inch square caps and footboards, each having a thickness of 0.223 in (Figure 5b). To reinforce the outer tube, a collar tube made from DOM1026 steel, measuring 1.540-in in thickness, with an outer diameter of 4.27 in and a wall thickness of 0.393 in, is welded into the outer tube (Figure 5c). The locking mechanism of Prop type-2 comprises 36 steel ball bearings, each with a diameter of 0.220 in, situated between the inner tube and the tapered surface of the outer tube (Figure 5c).

The Type-2 prop comprises a singular component, made from ASTM A500 Welded Grade C pipe. The pipe has an outer diameter of 3.5 in and a wall thickness of 0.25 in. Figure 6 shows a Type-2 prop before undergoing testing.

VERTICAL LOAD CAPACITY TESTS

The primary goal of vertical load tests is to establish a baseline performance (capacity and stiffness) for the tested props under static vertical loading conditions. In these tests, the props were positioned within the MRS, and a controlled vertical displacement was applied on the props at a slow rate of 0.05 in/min, simulating roof-to-floor convergence. The test naming conventions are outlined as follows: The initial segment of the test name denotes the type of prop being tested, with "T1" representing Type-1 props and "T2" representing Type-2 props. The subsequent part indicates the direction of loading, with "V" indicating vertical loading and "L" indicating lateral loading tests. Additionally, "L30" denotes a lateral loading test with a vertical pre-loading of 30 kips. The last segment indicates the prop height associated with the type of cape plate for Type-1 props.

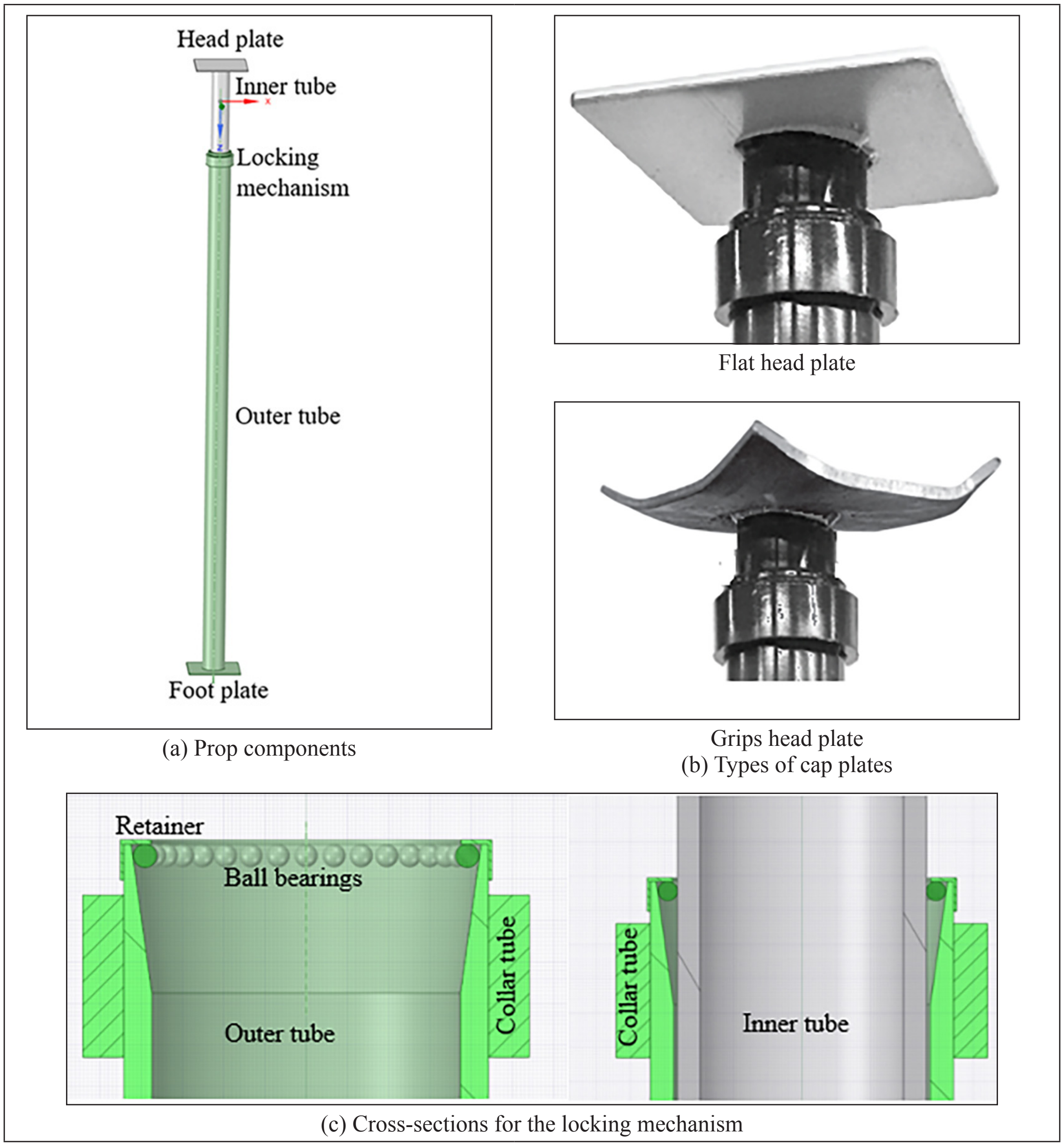

(a) Prop components

Flat head plate

Grips head plate
(b) Types of cap plates

(c) Cross-sections for the locking mechanism

Figure 5. Components for the locking mechanism

Two Type-1 props of 8-ft height were tested for vertical loading. Test T1-V-8F was conducted for a Type-1 prop with a flat head, while Test T1-V-8G was conducted for a Type-1 prop with a grips head plate (see Figure 5b). Figures 7a and 7b show the props configurations before and after testing. It shows that Type-1 props remain straight after vertical loading tests. Figure 7c shows the vertical load-displacement relationships for Type-1 props under vertical loading conditions. The tests of Type-1 props terminated at a vertical displacement of 8 in, although they could have been extended with constant vertical load capacity. In contrast to Test T1-V-8F, the load-displacement curve of Test T1-V-8G displayed an initial concave upward trend due to the deformation of its curved head plate. The purpose of the grips head plate was to grip into the roof, helping in securing it in place. The rigid MRS platens are not ideal for the Type-1 prop with grips head plate because this prop requires softer roof conditions. During the early loading stages, the curved head plate of T1-V-8G became flat, resulting in the prop achieving similar stiffness to Test T1-V-8F. However, it did not attain the same vertical load capacity. Both Type-1 props exhibited yielding behavior, with ultimate capacities of 110 kips and 140 kips, respectively. Consequently, the Type-1 props tested in this study are classified as "constant yielding" supports under pure vertical loading [6].

Three Type-2 props of varying heights (6 ft, 7 ft, and 8 ft) were tested. Figure 6a shows an 8-ft prop in its initial straight state before testing. Throughout the testing process, the floor platen of MRS gradually rose until the prop became unstable. At that point, the prop was unloaded gradually. Figure 6b illustrates the post-testing state of the prop, showing prop bended around its mid-height. Figure 8 shows the vertical load-displacement relationships of the tested Type-2 props. In Test T2-V-6, conducted with a 6-ft-tall prop, a peak vertical load of 191 kips was reached at a displacement of 0.34 in, then the vertical load was dropped to 100 kips. Test

(a) Prop before testing (b) Prop after testing

Figure 6. Type-2 prop (8-ft height) before and after experimental testing

Before After test Before After test

Tests T1-V-8F T1-V-8G

Figure 7. Vertical load results for Tests T1-V-8F and T1-V-8G (continues next page)

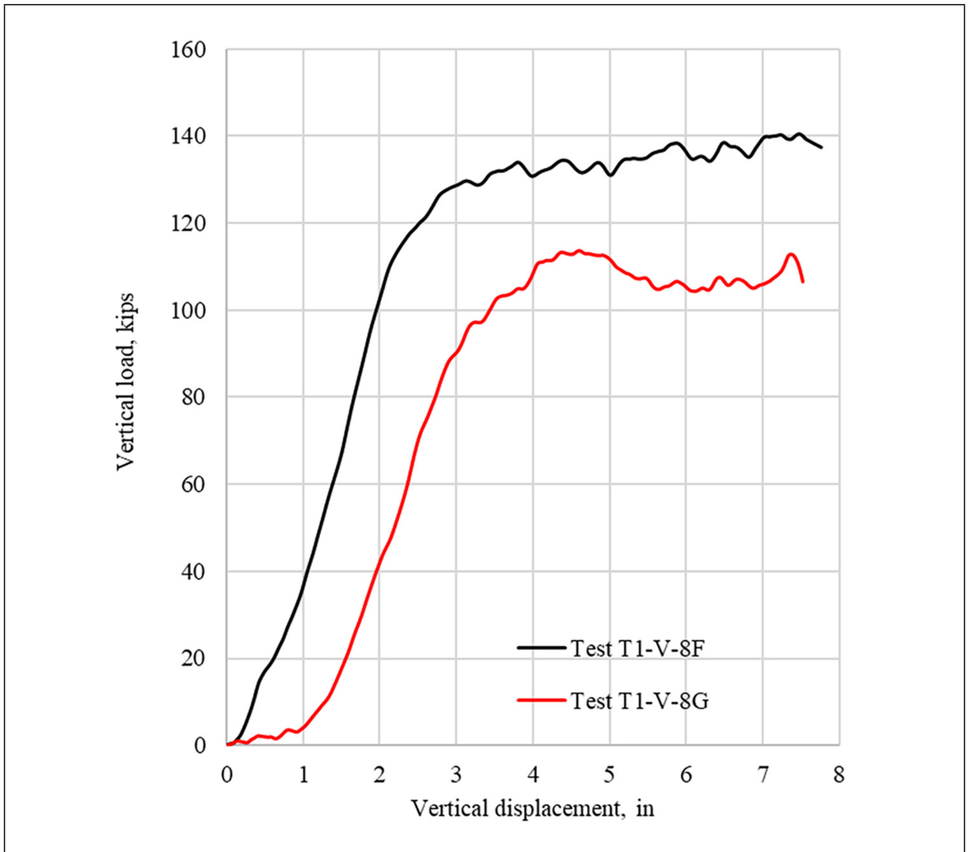

(c) Load-displacement curves

Figure 7. Vertical load results for Tests T1-V-8F and T1-V-8G (continued)

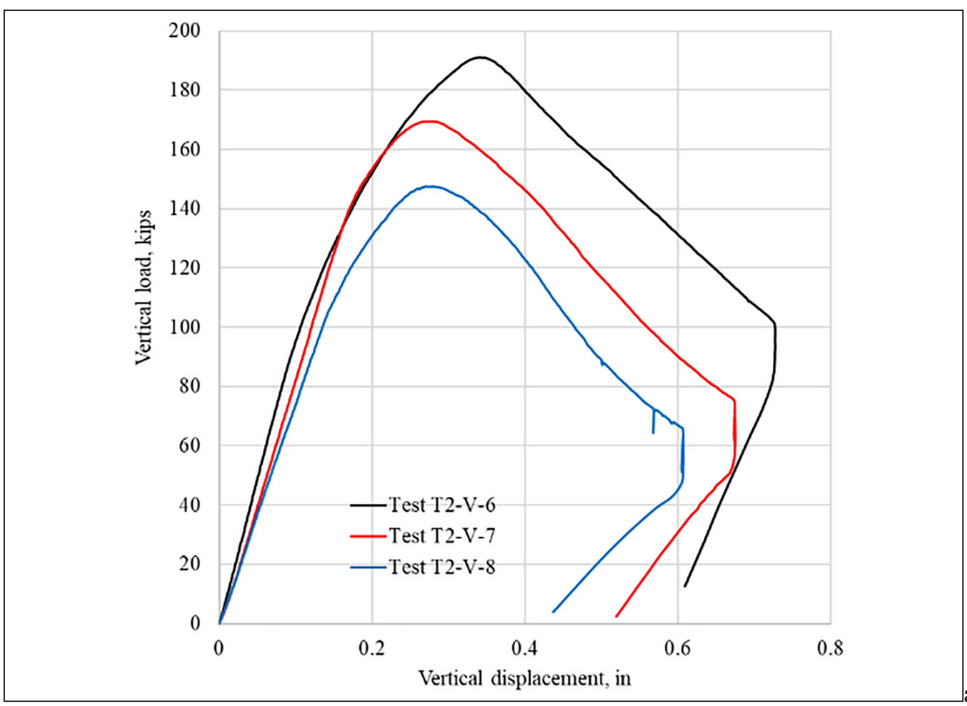

a

Figure 8. Vertical load-displacement curves tests for Type-2 props

T2-V-7, employing a 7-ft-tall prop, achieved a peak vertical load of 169 kips at a displacement of 0.28 in. Test T2-V-8, utilizing an 8-ft prop, resulted in a peak vertical load of 148 kips at a displacement of 0.28 in. Consequently, the tested Type-2 props are categorized in this study as "load shedding" supports [6].

Buckling analysis for the tested props under vertical load

Compression members, such as tested Type-1 and Type-2 props, may encounter failure through either material yielding or structural instability, commonly referred to as buckling. Euler's buckling theory offers a method to predict buckling of compression members such as studied props (see Equation 2). Buckling occurs for compression members when the applied compressive load exceeds a certain critical value, P_{cr}:

$$P_{cr} = \frac{\pi^2 EI}{(k \times L)^2} \quad (1)$$

where E is the Young modulus of steel material, I is moment of inertia of the prop's cross-sectional area, L denotes the length of the prop and k is a constant determined by the type of constraints at both ends of the prop, with a value of 0.5 for the tested props.

To apply Euler's buckling equation, the slenderness ratio (S) of long compression member must exceed the critical ratio, S_{crit}.

$$S = \frac{k \times L}{\sqrt{\frac{A}{I}}} \quad (2)$$

$$S_{crit} = \sqrt{(\pi^2 \times E/\sigma_u)} \quad (3)$$

where σ_u is ultimate strength of steel material and A refer to the cross-sectional area of the prop.

The Type-1 props did not exhibit buckling behavior in compression tests (see Figure 7). Therefore, buckling analysis was solely conducted for Type-2 props. The slenderness ratios for the 6-ft, 7-ft, and 8-ft Type-2 props have been determined as 31, 36, and 42, respectively. The critical slenderness ratio of the prop was determined to be 56. These findings indicate that the Euler buckling theory (Equation 1) is inadequate for calculating the critical buckling loads of Type-2 props. Instead, finite element modeling [7] was utilized to calculate the critical buckling loads. Further details regarding the used model can be found in Mohamed, and Batchler 2022 [5]. Table 1 presents a summary of both the measured peak loads and calculated critical buckling loads, along with their corresponding vertical displacements. Analysis of the table reveals that the computed critical buckling loads closely align with the measured peak loads, exhibiting a maximum difference percentage of 6%. These findings strongly suggests that the failure of the Type-2 props under testing conditions resulted from buckling rather than material yielding.

LATERAL LOAD CAPACITY TESTS

In this study, lateral loading tests are conducted to measure the lateral loading capacity of the props under study. Additionally, these tests aim to evaluate how lateral loading impacts their rated vertical loading capacity and yielding mechanisms. This study assumes that the effect of rib fall on the prop does not cause any dynamic loading.

To apply lateral loads to the tested props, a lateral loading fixture was bolted into the floor platen of the MRS (see Figure 9). This fixture utilized a hydraulic cylinder mounted on the lateral loading fixture to apply the lateral force. The height of the fixture is about 6-ft high, and the position of the hydraulic cylinder is adjustable so that the lateral load can be applied at the mid-height of the tested prop.

The lateral loading tests were conducted in three stages. In the first stage, the prop was loaded vertically with a predetermined percentage of its vertical load capacity. In the second stage, the prop was subjected to lateral loading at its mid-height until it dislodged, and the lateral loading vanished. In the third stage, the prop was again re-loaded vertically without lateral loading until it completely yielded. The second and third stages of lateral loading replicate scenarios in which friable or blocky sloughed ribs lean against the

(1) Lateral loading fixture mounted on the floor of the MRS
(2) Hydraulic loading ram (3) Tested Type-1 prop
(4) String pot (5) Tripod

Figure 9. Setup for lateral loading tests

Table 1. Critical buckling load and corresponding vertical displacement

Test ID	Prop Height, ft	Critical Buckling Load, kips			Vertical Displacement at Critical Load, in.		
		Test	Model	Difference %	Test	Model	Difference %
Test T2-V-6	6	191	179	–6%	0.34	0.33	–3%
Test T2-V-7	7	169	166	–2%	0.28	0.31	13%
Test T2-V-8	8	148	156	6%	0.28	0.30	7%

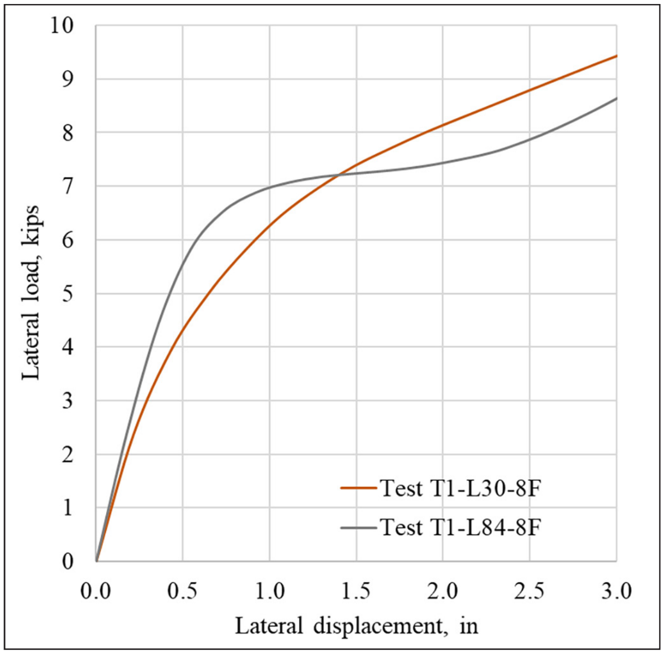

Figure 10. Lateral load-displacement curves for Tests T1-L30-8F and T1-L84-8F

prop, resembling a situation where a collapsed rib exerts lateral pressure on the prop before disintegrating, thus releasing lateral load while the prop supports the mine roof.

Two Type-1 props, each 8 feet tall with flat head plates, were subjected to lateral loading tests. In the first stage of lateral loading test, a vertical load of 30 kips (approximately 20% of the prop's load capacity) was applied in Test T1-L30-8F. In the second stage, a gradually increased lateral load was applied at the mid-height of the prop. The prop showed a lateral loading capacity of about 8.5 kips with 3 in of lateral displacement (Figure 10). Upon reaching its ultimate lateral loading capacity, the prop experienced a sudden drop in lateral load. The second test, Test T1-L84-8F, followed a similar procedure to the first, except for applying a higher vertical of about 84 kips (around 60% of the prop's load capacity). Under this condition, the prop showed a lateral loading capacity of about 9 kips (Figure 10). The lateral capacity of both Tests T1-L30-8F and T1-L84-8F converged to about 9 kips, which represents approximately 6% of its vertical loading capacity.

Figure 11 shows the post-testing configurations and vertical load-displacement curves for Type-1 props during the third stage of lateral loading testing. In this stage, vertical loading was continued until the props became unstable, at which point the tests were terminated with a vertical displacement of about 3.5 in. Upon final configurations, the props showed buckling at its mid-height with a lateral displacement of about 6.5 in (see Figures 11a and 11c). Figure 11c shows the vertical load-displacement curves for Tests T1-L30-8F and T1-L84-8F, along with the curve for Test T1-V-8F. In the first stage, the vertical load-displacement curves of Tests T1-L30-8F and T1-L84-8F coincided with that of Test T1-V-8F. During the second stage, the vertical loads applied on Tests T1-L30-8F and T1-L84-8F were vanished. In the third stage, the vertical load-displacement curves of Tests T1-L30-8F and

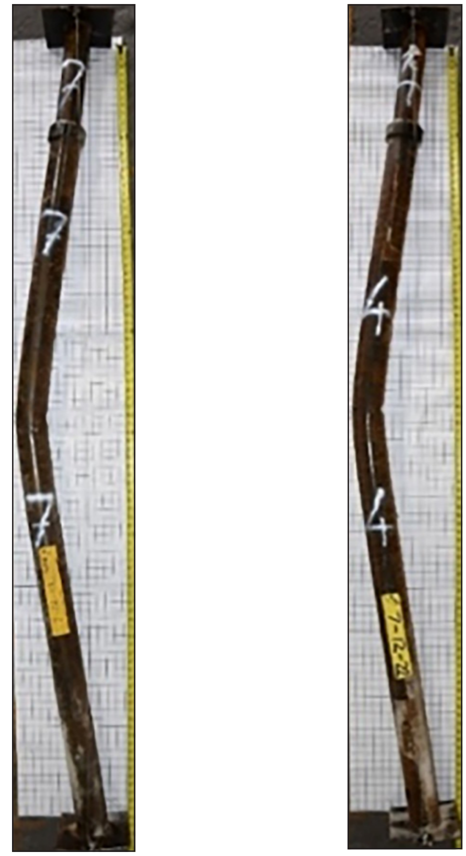

(a) T1-L30-8F (b) T1-L70-8F

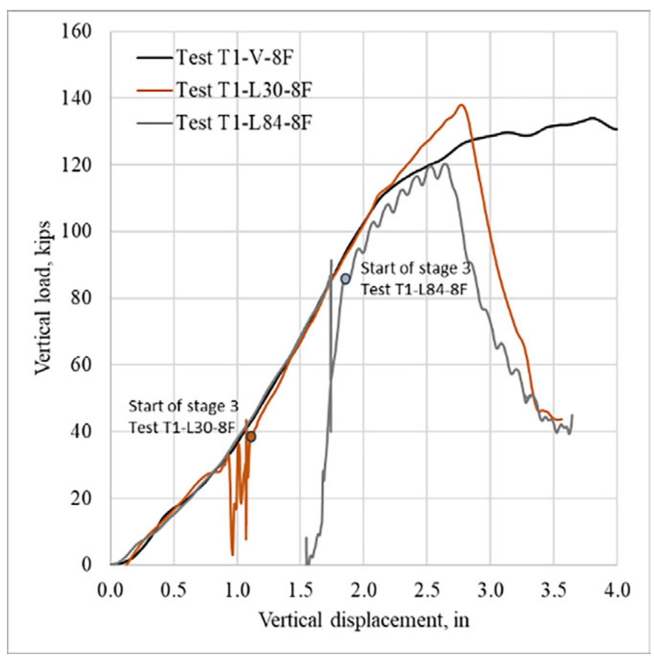

(c) Load-displacement curves

Figure 11. Vertical load results for Tests T1-L30-8F and T1-L84-8F

T1-L84-8F closely followed that of Test T1-V-8F, reaching vertical peak loads of 120 kips and 140 kips, respectively, before dropping to a residual vertical load capacity of approximately 40 kips. As previously described, the Type-1 props were classified as "constant yielding" supports under pure vertical loading. Figure 11c shows that when Type-1 props subjected to lateral loading, these props would be classified as "load shedding" supports.

Two Type-2 props, each measuring 8 ft in heigh, subjected to lateral loading tests. It was not planned to carry out the third stage of lateral loading during the preparation for the Type-2 props testing. In the first test, Test T2-L13-8, 0.5-inch-thick plywood boards were positioned at both the top and base of the prop (see Figure 12a). In the first stage, the prop was subjected to a vertical load of 13 kips. In the second stage, horizontal loading was incrementally applied until the prop slipped at a lateral load of 6.3 kips (as indicated by the solid red curve in Figure 13a) and a lateral displacement of 1.15 in. During this test, the initial vertical load could not be sustained at the designated 13 kips level (solid black curve see, Figure 13a), likely due to its relatively low magnitude, potentially falling within the margin of error of the MRS. However, the measurement of lateral loading, conducted through a load cell, was notably more consistent and controlled.

In the second test, Test T2-L20-8, plywood boards were placed at the top and base of the prop. However, in this test, horizontal movement of the top and bottom ends of the propas were constrained by steel blocks (see Figure 12b). Similar lateral loading procedure of the first test was applied in the second test, except for a slightly higher vertical load of about 20 kips applied in the second test. Under these conditions, the prop showed a lateral loading capacity of approximately 10.79 kips, as indicated by the solid red curve in Figure 13b, at a lateral displacement of 3.57 in. In the second stage of lateral loading, as the prop subjected to lateral force, it bended and formed an arch between the MRS platens. This arching mechanism, coupled with rigid MRS platens, explains the prop's capability to withstand the initial vertical load of 20 kips, then raise its vertical load capacity to about 33 kips (see the solid black curve in Figure 13b). As the tested prop undergoes additional lateral displacement, its vertical load capacity gradually diminishes until it reaches zero.

As previously mentioned, the third stage of lateral loading was not conducted for Type-2 props testing. Consequently, calibrated Finite Element (FE) models were employed to predict the responses of Type-2 props during this stage. Further details regarding the calibrated model for Type-2 props can be found in Mohamed, and Batchler 2022 [5]. Figure 13 shows the calibrated modeling results of Type-2 props models (shown as dotted lines in Figure 13), comparing them with the corresponding test results. In the simulation, the 0.5-inch-thick plywood boards at the top and base of the prop models were excluded. This simplification may result in an over-prediction of support vertical loads, particularly in simulating Test T2-L13-8, which had a small initial vertical load of about 13 kips. However, the predicted lateral load capacities for Tests T2-L13-8 and Test T2-L20-8 align with the actual test results.

Figure 14 shows the FE predictions of the vertical load-displacement and lateral load-displacement curves for Tests T2-L13-8 (model) and T2-L20-8 (model). The predicted vertical load-displacement curves are compared with Test T2-V-8, as shown in Figure 14b. The FE simulation was conducted in three steps:

Step 1: The prop models for Tests T2-L13-8 (model) and T2-L20-8 (model) were subjected to vertical loads of 13 kips and 20 kips, respectively, without any lateral load. This was achieved by displacing the bottom platen upward while keeping the upper platen stationary.

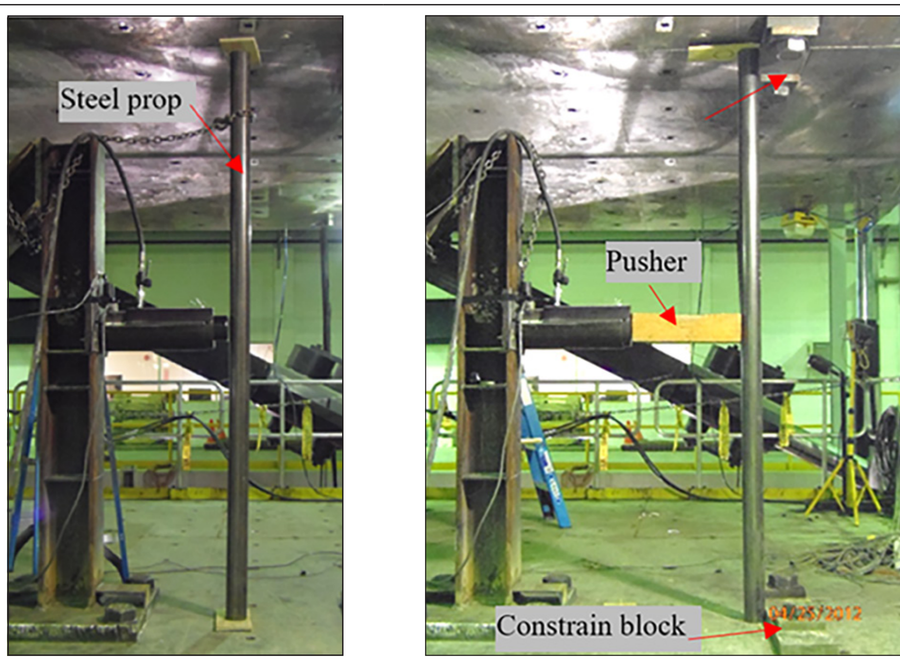

Test T2-L13-8 Test T2-L20-8

Figure 12. Setup for testing Type-2 props

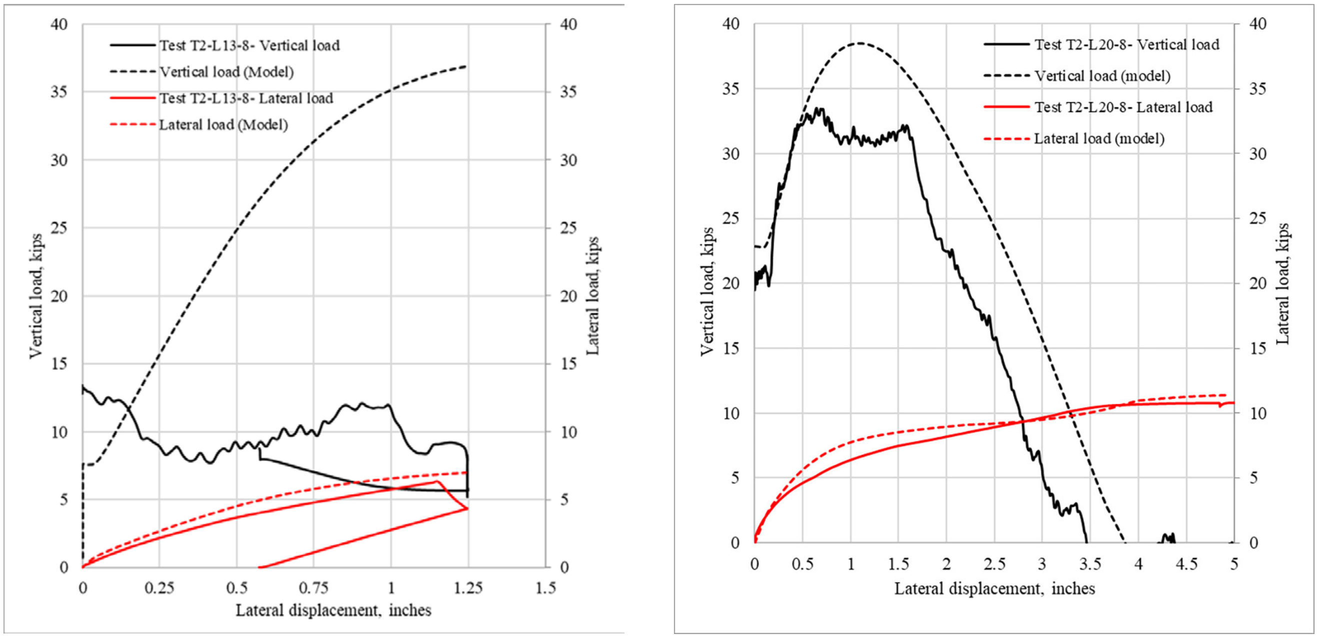

(a) Test T2-L13-8 (b) T2-L20-8

Figure 13. Experimental and Finite Element (FE) modeling load-displacement curves for Type-2 props

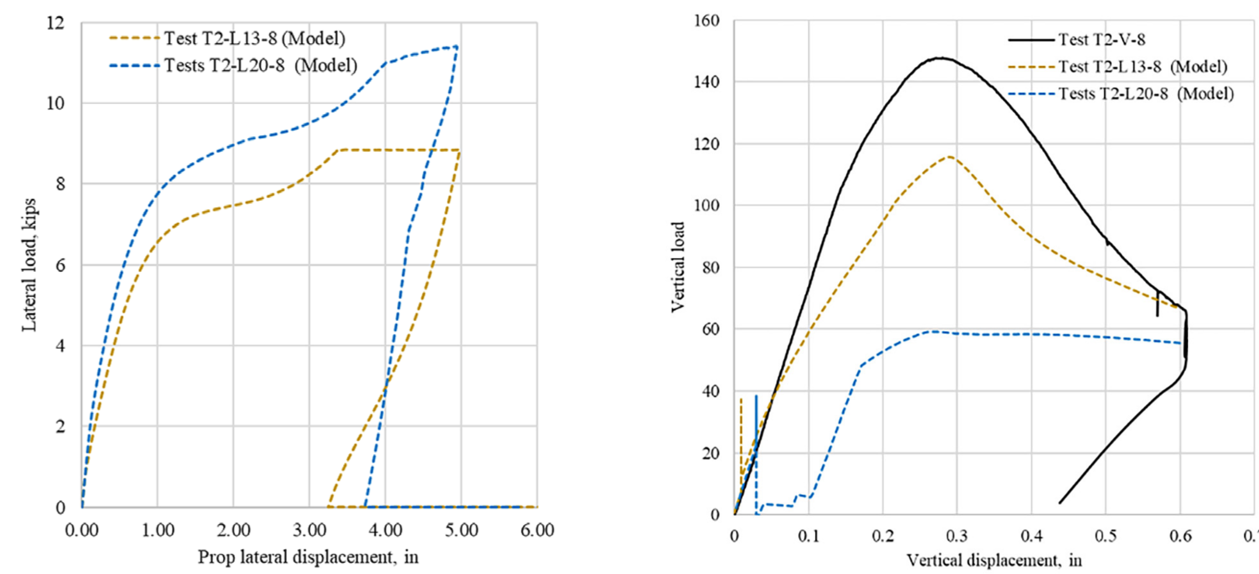

(a) Lateral load-displacement curve (b) Vertical load-displacement curve

Figure 14. Predicted load-displacement curves for Type-2 props during stage 3 of lateral loading

Step 2: The prop models were laterally loaded at the mid-height with a displacement of 5 in, while the top and bottom platens were held stationary. The predicted ultimate lateral resistance at this stage was approximately 8.8 kips and 11.4 kips for Tests T2-L13-8 (model) and T2-L20-8 (model), respectively (Figure 14a).

Step 3: The prop models were unloaded laterally while vertical loading resumed, resulting in a total vertical displacement of 0.6 inches. In Test T2-L13-8 (model), the vertical load increased to about 115 kips, then decreased to about 66 kips, while the lateral load decreased to zero. The retained residual vertical loading capacity for Test T2-L13-8 (model) is about 44% of that seen in Test T2-V-8 (Figure 14b). In Test T2-L20-8 (model), the prop achieved a constant vertical load capacity of about 60 kips, representing about 40% of the capacity observed in Test T2-V-8. As previously described, Type-2 props were categorized as "load shedding"

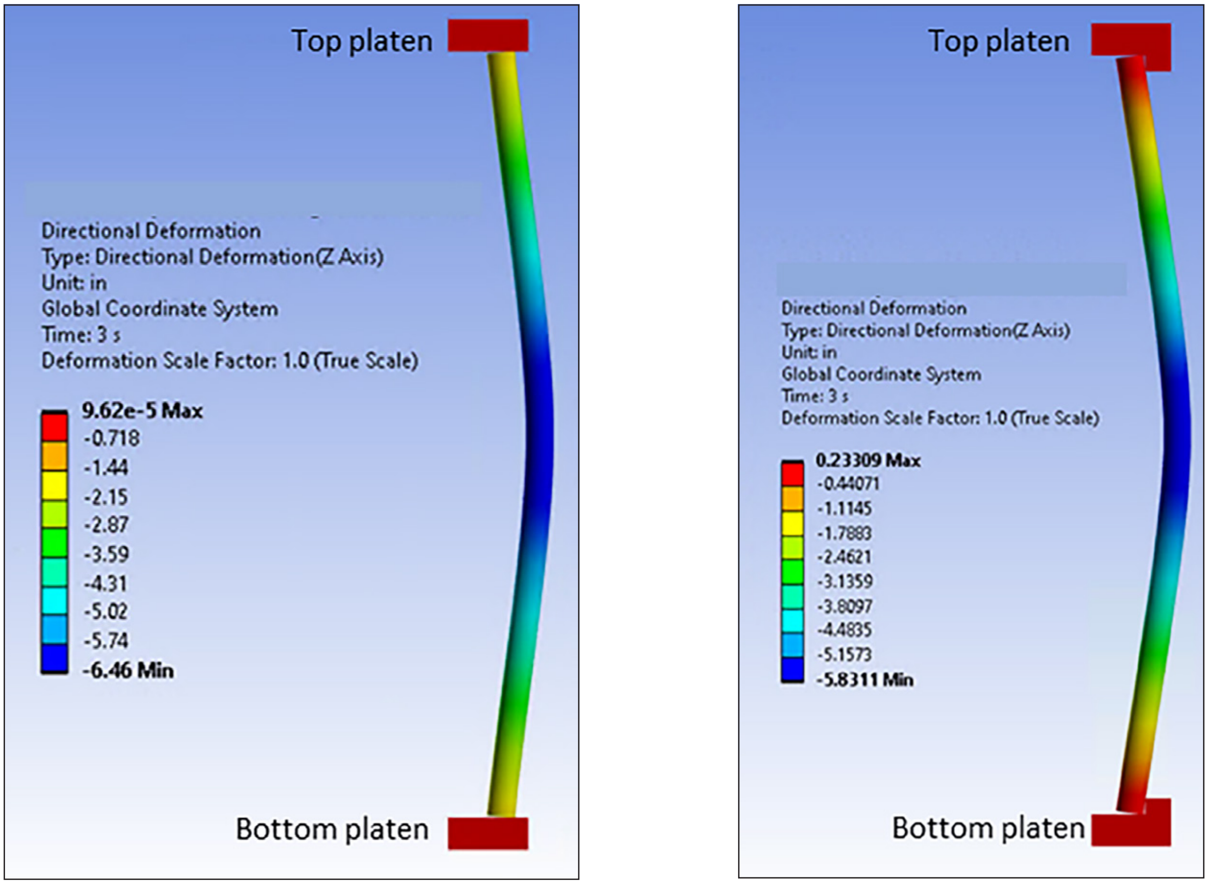

(a) Test T2-L13-8 (b) Test T2-L20-8

Figure 15. Type-2 props total deformation during stage 3 of lateral loading

supports under pure vertical loading. Figure 14b shows that Test T2-L13-8 maintains this characteristic under lateral loading with lower vertical loading capacity. In contrast, Test T2-L30-8 would be classified as a "constant yielding" support with lower vertical loading capacity when subjected to lateral loading.

SUMMARY AND CONCLUSIONS

Minimal research exists on the performance of standing support systems against lateral loads. NIOSH initiated a testing program to assess various standing supports' lateral loading capacities, involving samples from research collaborators. This study aims to measure the lateral loading capacity of tested props and its impact on vertical loading capacity and yielding mechanisms. It uses the MRS at NIOSH Pittsburgh to test two types of standing supports: Type-1 with telescopic tubes made from ASTM A-513 steel, and Type-2 with a singular component made from ASTM A500 Welded Grade C pipe.

Vertical load tests were conducted to assess the performance of Type-1 and Type-2 props under controlled loading conditions simulating roof-to-floor convergence. Type-1 props, with flat or grips head plates, showed "constant yielding" behavior with ultimate capacities of 110 kips and 140 kips, respectively. While the grips head plate initially deformed, it eventually achieved similar stiffness to the flat head plate but with lower load capacity due to its design. Type-2 props of different heights showed a "load shedding" pattern, with peak vertical loads ranging from 148 kips to 191 kips before unloading.

The Type-1 props did not exhibit buckling behavior in compression tests. Therefore, buckling analysis was solely conducted for Type-2 props. The critical buckling loads of Type-2 props were determined using finite element modeling, aligning closely with measured peak loads. This indicates that the Type-2 props failed due to buckling, not material yielding.

Lateral loading tests were conducted on two Type-1 props to measure their lateral loading capacities when subjected to predetermined initial vertical loads. Lateral load capacities of Type-1 props converged to about 9 kips (6% of vertical capacity). This study revealed that while Type-1 props were initially considered "constant yielding" supports under vertical loads, the introduction of lateral loading reclassified them as "load shedding" supports. It was observed that under lateral loading, these props could not sustain their rated vertical loading capacity. Instead, they retained a residual vertical load capacity of 40 kips (29% of vertical capacity).

Two Type-2 props, each 8 ft tall, underwent testing to determine their lateral load capacities under different initial vertical loads. The results indicated a maximum lateral load capacity of 6.3 kips for

Test T2-L13-8 and 10.79 kips for Test T2-L20-8. To estimate the retained vertical loading capacity and loading behavior of Type-2 props, calibrated FE models for Type-2 props were developed. Type-2 props were categorized as "load shedding" supports under pure vertical loading. The modeling results indicated that while lateral loading did not affect the loading mechanism of Test T2-L13-8, it did reduce its rated vertical loading capacity. The retained a residual vertical load capacity of 66 kips (44% of vertical capacity). In contrast, the lateral loading affected the loading behavior of Test T2-L30-8, causing the prop to be reclassified as a "constant yielding" support with a reduced vertical load capacity of 60 kips (40% of its original vertical capacity).

STUDY LIMITATIONS

The findings in this research are limited to the tested props and their specific dimensions and properties. The study also reflects the impact of rigid MRS patens on prop response. However, there remain several areas that warrant further investigation. For instance, do the end-conditions, such as steel platens versus strong/weak synthetic rocks, affect the vertical loading capacity of steel props? Does the spatial location of the lateral load along the support influence its lateral loading capacity? Furthermore, it is essential to test other types of support structures. Ultimately, the information gleaned from this study and future research endeavors can inform the development of rib design criteria and aid mine operators in selecting and utilizing rib support in underground mines.

DISCLAIMER

The findings and conclusions in this study are those of the authors and do not necessarily represent the official position of the National Institute for Occupational Safety and Health (NIOSH), Centers for Disease Control and Prevention (CDC). Mention of any company or product does not constitute endorsement by NIOSH.

REFERENCES

MSHA (2010) Report of investigation. Fall of roof/rib. CAI-2010–38.

Spearing S (2008) Designing Free-Standing Steel Supports for Coal Mine Roof Support. 27th International Conference on Ground Control in Mining (ICGCM).

Chen Y, Pu H, Wu P, Wu H, Wu Y, Hao Y, Lai GT, Azmi A, and Abdurrahman M (2020) Mechanical properties experiment of load capacity on a mechanical yielding steel prop (MYSP) and its application in roadway support. http://dx.doi.org/10.17576/jsm-2020-4907-05.

Barczak TM and Tasillo Carol L (1988) Factors affecting strength and stability of wood cribbing: height, configuration, and horizontal displacement. Report of investigations (United States Bureau of Mines), 9168.

Mohamed KM and Batchler T (2022) Analysis of steel prop supports subjected to vertical and lateral loading. Mining, Metallurgy & Exploration, doi:10.1007/s42461-022-00673-2.

Barczak TM. An overview of standing roof support practices and developments in the United States. In: Proceedings of the Third South African rock engineering symposium. Johannesburg, Republic of South Africa: South African Institute of Mining and Metallurgy; 2005 p. 301–34.

ANSYS (2020) Documentation for ANSYS, release 20. ANSYS Inc., Canonsburg, PA.

PROCEEDINGS OF THE 43rd International Conference ON GROUND CONTROL IN MINING

ICGCM 2024

Edited by

Ted Klemetti | Rudrajit Mitra | Michael Murphy | Kyle Perry | Ihsan Berk Tulu

SME Society for Mining, Metallurgy & Exploration®

Society for Mining, Metallurgy & Exploration (SME)
12999 E. Adam Aircraft Circle
Englewood, Colorado, USA 80112
(303) 948-4200 / (800) 763-3132
www.smenet.org

The Society for Mining, Metallurgy & Exploration (SME) is a professional society whose more than 15,000 members represents all professionals serving the minerals industry in more than 100 countries. SME members include engineers, geologists, metallurgists, educators, students and researchers. SME advances the worldwide mining and underground construction community through information exchange and professional development.

ebook ISBN 978-0-87335-516-2